Operational Head-on Beam-Beam Compensation with Electron Lenses in the Relativistic Heavy Ion Collider

W. Fischer, X. Gu, Z. Altinbas, M. Costanzo, J. Hock, C. Liu, Y. Luo, A. Marusic, R. Michnoff, T. A. Miller, A. I. Pikin, V. Schoefer, P. Thieberger, and S. M. White

Phys. Rev. Lett. **115**, 264801 — Published 23 December 2015

DOI: 10.1103/PhysRevLett.115.264801

Operational head-on beam-beam compensation with electron lenses in the Relativistic Heavy Ion Collider

W. Fischer,* X. Gu, Z. Altinbas, M. Costanzo, J. Hock, C. Liu, Y. Luo, A. Marusic, R. Michnoff, T.A. Miller, A.I. Pikin, V. Schoefer, and P. Thieberger
Brookhaven National Laboratory, Upton, NY 11973, USA

S.M. White
European Synchrotron Radiation Facility, BP 220, 38043 Grenoble Cedex, France

Head-on beam-beam compensation has been implemented in the Relativistic Heavy Ion Collider (RHIC) in order to increase the luminosity delivered to the experiments. We discuss the principle of combining a lattice for resonance driving term compensation and an electron lens for tune spread compensation. We describe the electron lens technology and its operational use. To date the implemented compensation scheme approximately doubled the peak and average luminosities.

PACS numbers: 29.20.db, 29.27.Bd, 45.20.Jj

The particle motion in storage ring colliders can be well described by Hamiltonian mechanics, where the formalism is applicable over the time scale of possible damping mechanisms such as radiation damping in lepton machines. The stability of motion in Hamiltonian systems is limited by nonlinearities, and in colliders the strongest nonlinearities that a particle experiences are typically created by the electromagnetic fields when passing through the other beam. This head-on beam-beam interaction gives rise to resonance driving terms and widens the tune distribution thereby limiting the achievable beam lifetime and luminosity, as is the case in polarized proton operation in RHIC.

The strength of the head-on beam-beam effect is parameterized by the beam-beam parameter ξ_p, the tune shift experienced by a small amplitude particle due to the electromagnetic forces of the other beam in an interaction point (IP). The beam-beam parameter for proton-proton collisions is $\xi_p = -(r_p N_p)/(4\pi\epsilon_n)$, where r_p is the classical proton radius, N_p the bunch intensity, and $\epsilon_n = (\beta_p\gamma_p)\sigma_p^2/\beta$ the normalized rms emittance. $(\beta_p\gamma_p)$ are the relativistic factors of the proton beam, σ_p is the transverse rms beam size and β the lattice function. ξ_p is independent of the beam energy. In beam-beam limited colliders with round Gaussian beams at the IP like RHIC, the luminosity can be written as [1]

$$\mathcal{L} = \frac{f_c}{4\pi}\frac{N_p^2}{\sigma_p^{*2}}H = \frac{4\pi f_c}{r_p^2}\frac{(\beta_p\gamma_p)\epsilon_n}{\beta^*}H\xi_p^2 \qquad (1)$$

where f_c is the collision frequency, σ_p^* the beam size at the IP, H a geometric factor ≤ 1 that accounts for the hourglass effect and crossing angles, and β^* the lattice function at the IP. Due to the quadratic dependence of the luminosity $\mathcal{L}$ on the beam-beam parameter ξ_p, gains in ξ_p implemented through an increase in N_p at constant ϵ_n translate into more than twice the gains in $\mathcal{L}$.

* Wolfram.Fischer@bnl.gov

Soon after the first colliders went into operation in 1962 [2], compensation of the head-on beam-beam effect was contemplated. The first and only scheme implemented until now was the 4-beam collider DCI in the 1970s with 2 electron and 2 positron beams, all meeting at the same interaction point [3]. With the beam-beam space charge forces eliminated a luminosity increase of up to two orders of magnitude was expected. The compensation was not successful due to the unexpected coherent motion of the beams [4], and the luminosity in 2-, 3-, or 4-beam operation was about the same [3]. Later, head-on beam-beam compensation with electron lenses was proposed for the SSC [5], Tevatron [6], and LHC [7].

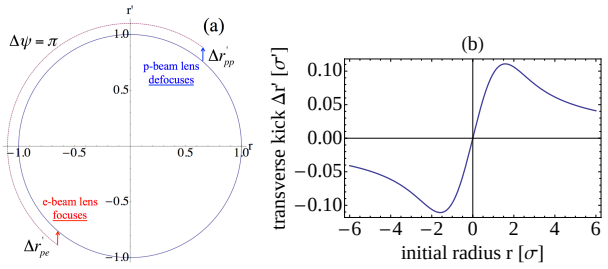

FIG. 1. (a) Head-on beam-beam compensation in a phase space view. A defocusing kick $\Delta r'_{pp}$ a proton receives from the other proton beam is reversed by a focusing kick $\Delta r'_{pe}$ from the electron lens after a phase advance π. (b) Amplitude dependence of the beam-beam kick $\Delta r'$ on the radius r.

Head-on beam-beam compensation (Fig. 1(a)) can be implemented in a single turn. We are using transverse phase space coordinates (r, r') with $r' = \frac{dr}{ds}$, s being the path length. The transverse kick $\Delta r'_{pp}$ that a particle receives when passing through the other beam is reversed in the same turn when the particle passes through a correction element and receives the kick $\Delta r'_{pe}$. Two conditions need to be fulfilled for exact compensation for all amplitudes r [8, 9]: (i) The correction element is placed at a phase advance of $k\pi$, k being an integer, after the beam-beam interaction in order to minimize the beam-beam resonance driving terms ($k = 0$ for DCI); (ii) The amplitude dependence of the correction kick $\Delta r'_{pe}(r)$ is

the same as for the beam-beam interaction, $\Delta r'_{pp}(r)$, in order to reduce the beam-beam induced tune spread.

For RHIC a lattice with a $k\pi$ phase advance between one IP and one of the two electron lenses was developed for both rings [10] and implemented [11], which had the added benefit of a larger off-momentum dynamic aperture than the previously used lattice. The tune spread reduction of the electron lens works as follows. For round bunches short compared to β^*, the kick $\Delta r'_{pp}$ is [12]

$$\Delta r'_{pp}(r) = +\frac{N_p r_p (1+\beta_p^2)}{\beta_p^2 \gamma_p r}\left[1-\exp\left(-\frac{r^2}{2\sigma_p^2}\right)\right]. \quad (2)$$

Figure 1(b) shows the non-monotonic amplitude dependence of $\Delta r'(r)$, which cannot be created with magnets. However, the same amplitude dependence can be created with another beam. In our case a low-energy electron beam stabilized in a longitudinal solenoid field is used, a device known as an electron lens (DCI used a high-energy beam). With the electron beam direction opposite to the proton beam, the electron lens creates a kick

$$\Delta r'_{pe}(r) = -\frac{2 n_e L_e r_p (1+\beta_p\beta_e)}{\beta_p^2 \gamma_p r}\left[1-\exp\left(-\frac{r^2}{2\sigma_e^2}\right)\right] \quad (3)$$

where n_e is the electron line density and L_e the length of the lens, β_e the relativistic factor of the electrons, and σ_e the rms electron beam size, also assumed to be Gaussian. For ultra-relativistic beams, $\beta_p \approx 1$, the compensation condition $\Delta r'_{pe}(r) = \mp \Delta r'_{pp}(\pm r)$ (different signs for k even or odd) is fulfilled for $\sigma_p = \sigma_e$ in the electron lens with an electron beam current of

$$I_e = \left(\frac{N_p}{L_e}\right)\frac{ec\beta_e}{1+\beta_e}. \quad (4)$$

The beam-beam parameters from the proton-proton and proton-electron collisions with $\xi_p = -\xi_e$ are then

$$\xi_p = -\frac{r_p}{4\pi}\frac{\beta^*}{(\beta_p\gamma_p)}\frac{N_p}{\sigma_p^{*2}} \quad \text{and}$$
$$\xi_e = +\frac{r_p}{4\pi}\frac{\beta_{el}}{(\beta_p\gamma_p)}\frac{(I_e L_e)}{\sigma_e^2}\frac{1+\beta_e}{ec\beta_e}, \quad (5)$$

where β_{el} is the lattice function at the electron lens. The operational implementation of the compensation principle requires an understanding of the tolerable deviations from the ideal case described above, and technical implementations within the allowable tolerances [8, 9].

Electron lenses were first used in the Tevatron [13, 14] where they cleaned the abort gap in operation [15], and demonstrated a better lifetime of bunches with long-range beam-beam effects [16]. Electron lenses with hollow electron beams were also tested as collimation devices [17]. The main parameters of the RHIC electron lenses (Fig. 2) [9, 18] are shown in Table I.

A major design consideration was the creation of a low-noise (DC) electron beam with a Gaussian transverse profile [18]. The electron beam is fully magnetized, i.e. it is transported along a solenoidal field from the electron gun to the collector. The stability of the electron beam during the interaction with the proton beam is provided by a superconducting solenoid with a field of up to 6 T [19]. The field lines deviate only ± 50 μm from straight lines, a fraction of the rms beam size in the lens (Table I), as studied in simulations [8], in order to maximize the overlap of the proton and electron beams.

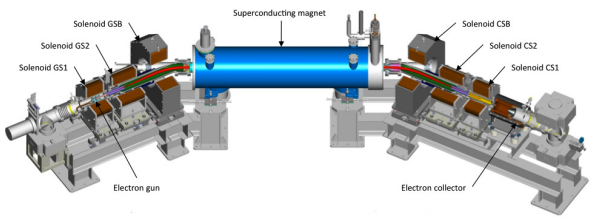

FIG. 2. One of two RHIC electron lenses. The electron beam moves from left to right and collides with the proton beam, moving from right to left, inside the superconducting solenoid.

TABLE I. Typical electron lens parameters for 2015 and design values (for up to 250 GeV proton energy).

quantity	unit	2015 value	design value
distance of center from IP10	m	— 3.3 —	
magnetic length L_e	m	— 2.4 —	
gun solenoid field B_g	T	0.31	≤ 0.69
main solenoid field B_m	T	5.0	$2-6$
cathode radius (2.7σ)	mm	7.5	4.1, 7.5
rms beam size in main solenoid σ_e	μm	650	≥ 300
kinetic energy E_e	keV	5.0	≤ 10
relativistic factor β_e	...	0.14	≤ 0.2
electron beam current I_e	mA	600	≤ 1000
beam-beam parameter from lens ξ_e	0.001	+10	$\leq +15$

Instrumentation is a critical part of the electron lens operation, as the position of both the electron and proton beam need to be monitored, and their overlap within a fraction of an rms beam size. This is reliably achieved with a novel monitor that detects electrons backscattered by the protons (Fig. 3) [20], and allows for a fast and robust alignment of the electron and proton beams.

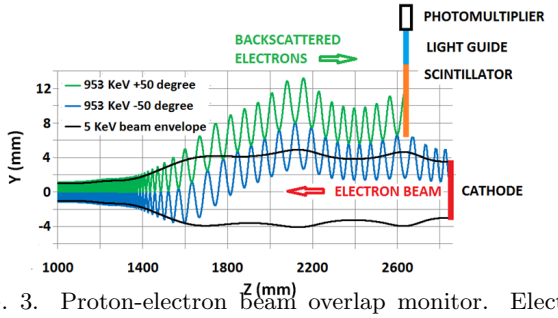

FIG. 3. Proton-electron beam overlap monitor. Electrons backscattered off protons are bent upwards in the GSB solenoid (see Fig. 2), pass through a 0.1 mm thin titanium alloy window and are detected with a scintillator [20].

The function of the electron lens is the reduction of the beam-beam induced tune spread. The tune distribution is measured with a transverse beam transfer function (BTF), which is the coherent response of the beam to a small harmonic dipole excitation of variable frequency Q.

In the absence of coherent modes the width of the tune distribution is given by the non-zero imaginary part of the complex BTF $R(Q)$, i.e. $\mathrm{Im}(R) > 0$ [21]. In RHIC coherent modes are not self-excited, not harmful to operation, and are almost unaffected by the electron lens. Although successful in simulations [22], the tune distribution widths could not be measured via the BTF if coherent beam-beam modes were present, as is the case in polarized p+p operation.

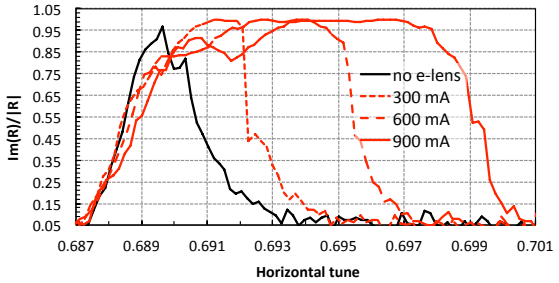

FIG. 4. Measured tune distribution as a function of the electron beam current without beam-beam collisions and with an electron beam size of $\sigma_e = 0.55$ mm. The curves are aligned to the left with an offset for better visibility of the effect.

However, the effect of the electron lens on the tune distribution was measured with proton beams without beam-beam collisions (Fig. 4), and with proton-aluminum beam-beam collisions (Fig. 5). Different from p+p operation, in p+Al operation the fractional tunes in the two beams differ by a value much larger than the beam-beam parameter ξ_p, and therefore the beams exhibit no coherent oscillation modes when excited.

Figure 4 shows that, as expected, the width of the horizontal tune distribution increases with increasing electron beam current. This tune spread is used to compensate the the beam-beam generated tune spread, which is shown in Fig. 5 with p+Al collisions. The tune spread is increased due to 2 beam-beam interactions, and decreased again with the electron lens.

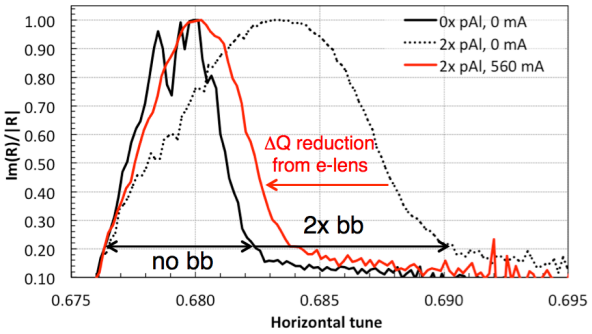

FIG. 5. Tune distribution width reduction with the electron lens, measured in the proton beam with p+Al collisions. The distribution widens due to two beam-beam interactions, and narrows again with the electron lens. The curves are aligned to the left with an offset for better visibility of the effect.

For operational use it was verified that the electron lenses do not introduce additional emittance growth, and only small additional beam losses (1-2%/h). The increased loss rate did not measurably affect the luminosity as it stems from particles in the tails that contribute little to the luminosity. For physics stores the electron lenses were turned on while the electron and proton beams were transversely separated and before the proton beams went into collision. Then collisions were established in one experiment, which allowed to set the collimators to store positions. In a second step the beams went into collision in the second experiment and the electron lenses simultaneously. Due to the tune compression, higher beam-beam parameters can be accommodated with the lenses. With too large beam-beam parameters ξ_p fast emittance growth or larger beam loss rates can be observed. After commissioning, 112 out of 156 p+p stores used both electron lenses, without any turn-on failure. One of the lenses exhibited unstable electron beam currents $\gtrsim 500$ mA leading to emittance growth in the proton beam. Its current was then limited to 430 mA, 30% lower than the electron beam current shown in Table I.

TABLE II. Main parameters for polarized proton operation at 100 GeV beam energy in 2012 (without) and 2015 (with head-on beam-beam compensation), and conditions for the maximum beam-beam parameters achieved in operation and tests in 2015 without and with electron lenses.

quantity	unit	operations (avg. over 10 best stores)		tests for max $\lvert\xi_p\rvert$		
		2012	2015	without e-lens	with e-lens	with e-lens
				— 2015 —		
bunch intensity N_p	10^{11}	1.6	2.25	2.6	2.15	2.0
no of bunche k_b	...	109	111	48	111	30
$\beta^*_{x,y}$ at IP6, IP8 (p+p)	m	0.85	0.85	— 0.85 —		
$\beta^*_{x,y}$ at e-lens (p+e)	m	10.5	15.0	— 15.0 —		
lattice tunes (Q_x, Q_y)	...	(0.695,0.685)		— (0.695,0.685) —		
rms emittance ϵ_n	μm	3.3	2.8	3.5	2.4	1.9
rms beam size IP6/8 σ^*_p	μm	165	150	170	150	125
rms beam size e-lens σ_p	μm	—	630	700	645	520
rms bunch length σ_s	m	0.63	0.70	0.77	0.70	0.56
hourglass factor H	...	0.74	0.75	0.78	0.81	0.86
beam-beam param. ξ_p/IP	0.001	−5.8	−9.7	−9.1	−10.9	−12.6
# of beam-beam IPs	...	2	2+1*	2	2+1*	2+1*
luminosity $\mathcal{L}_{peak}$	$10^{30}\mathrm{cm}^{-2}\mathrm{s}^{-1}$	46	115	72	115	40
luminosity $\mathcal{L}_{avg}$	$10^{30}\mathrm{cm}^{-2}\mathrm{s}^{-1}$	33	63	—	—	—

* One p+p collision in IP6 and IP8, and a compensating p+e collision in IR10.

Table II shows the main operational parameters in 2012 without beam-beam compensation and in 2015 with compensation, as well as parameters for maximum ξ_p reached in operations with 111 bunches, and tests with 30 and 48 bunches. With fewer bunches brighter beams can be created. In RHIC only 1 of the 2 beam-beam interactions is to be compensated. This provides enough luminosity gain for the upgrade goals and leaves enough tune spread for beam stabilization. In operation the maximum beam-beam parameter increased by 67%, and the peak and average store luminosities by 2.5× and 1.9× respectively. Further increases in the luminosity were limited by the bunch intensity and brightness available from the injector.

The maximum achievable beam-beam parameter ξ_p with lenses was determined with operational data, and with and without lenses in tests with fewer but brighter bunches. To determine the maximum ξ_p under different conditions, both the emittance and the relative beam loss need to remain below a certain limit. Figure 6 shows the

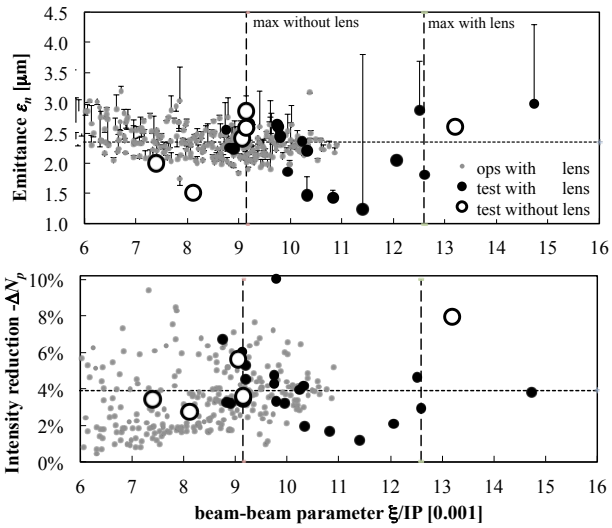

FIG. 6. Top: initial emittance and its increase after 5 min (vertical lines) as a function of the beam-beam parameter. Bottom: reduction in the bunch intensity N_p over 5 min.

initial emittance, its increase after 5 min (top) and the relative beam loss over 5 min both as a function of the beam-beam parameter. The horizontal dashed lines are averages from the distribution of good operational stores, vertical lines mark the maximum demonstrated ξ_p without and with lenses. Parameters of the cases with lenses are also shown in Table II.

The maximum demonstrated beam-beam parameter achieved without e-lenses is $\xi_p = -0.0091$. The best operational stores with e-lenses reached $\xi_p = -0.0109$ (+20% in $|\xi_p|$), and a test reached -0.0126 (+38% in $|\xi_p|$) (Table II). Note that it is possible that higher beam-beam parameters can be demonstrated in the future in all situations thereby changing the relative gains. For the cases with e-lenses, the achievable ξ_p was limited by the intensity and brightness available from the injector.

The head-on beam-beam compensation implemented in RHIC, consisting of a new lattice and an electron lens in each ring with transversely Gaussian electron beam, increased the peak and average luminosities by approximately a factor of two. A limited number of tests to demonstrate the highest possible beam-beam parameter $|\xi_p|$ showed an increase by +38% through the use of the electron lens, limited by the available brightness from the injectors. Therefore, with upgrades in the injector chain even higher beam-beam parameters and luminosities can be expected.

The work was supported by many in the Collider-Accelerator Department, and the Superconducting Magnet Division at Brookhaven National Laboratory. The authors are also thankful for discussions and support to V. Shiltsev, A. Valishev, T. Sen, and G. Stancari, FNAL, who generously shared the Tevatron experience with us; N. Milas, LNLS; X. Buffat, R. DeMaria, U. Dorda, W. Herr, J.-P. Koutchouk, T. Pieloni, F. Schmidt, and F. Zimmerman, CERN; K. Ohmi, KEK; V. Kamerdziev, FZ Jülich; A. Kabel, SLAC and P. Görgen, TU Darmstadt. We are thankful to the US LHC Accelerator Research Program (LARP) for support of beam-beam simulations. Work was supported by Brookhaven Science Associates, LLC, under Contract No. DE-AC02-98CH10886 with the US Department of Energy.

[1] M.A. Furman and M.S. Zisman, in "Handbook of accelerator physics and engineering", 2nd ed., World Scientific, pp. 311-318 (2013).
[2] K. Oide, Reviews of Accelerator Science and Technology, Vol. 7, pp. 35-48 (2014).
[3] G. Arzelia et al., Proc. 8th Int. Conf. High Energy Acc., pp. 150 (1971); M. Bergher et al., proc. 1979 Part. Accel. Conf., San Francisco, CA, USA, pp. 3559-3561 (1979).
[4] Ya.S. Derbenev, Nuclear Physics Institute, Siberian Division, Academy of Sciences USSR, Novosibirsk, Report No IYAF 70-72, in Russian (1972), SLAC-TRANS 151 in English; B. Podobedov and R.H. Siemann, Phys. Rev. E 52, No 3, pp. 3066-3073 (1995).
[5] E. Tsyganov, R. Meinke, W. Nexsen, A. Zinchenko, SSCL-PREPRINT-519 (1993).
[6] V. Shiltsev et al., Phys. Rev. ST Accel. Beams 2, 071001 (1999).
[7] E.N. Tsyganov, A. Taratin, and A.I. Zinchenko, CERN SL-Note-95-116-AP (1995).
[8] Y. Luo et al., Phys. Rev. ST Accel. Beams 15, 051004 (2012).
[9] W. Fischer et al., proc. ICFA Mini-Workshop on Beam-Beam Effects in Hadron Colliders (BB3013), CERN, CERN-2014-004, pp. 109-120 (2014).
[10] S. White, W. Fischer, and Y. Luo, BNL-105550-2014-IR, C-A/AP/519 (2014).
[11] V. Schoefer et al., International Particle Accelerator Conference 2015, Richmond, VA, USA, pp. 2384-2386 (2015)
[12] E. Keil, in CERN 95-06, pp. 539-555 (1995).
[13] V. Shiltsev and A. Zinchenko, Phys. Rev. ST Accel. Beams 1, 064001 (1998).
[14] V. Shiltsev et al., Phys. Rev. ST Accel. Beams 11, 103501 (2008).
[15] X.-L. Zhang et al., Phys. Rev. ST Accel. Beams 11, 051002 (2008).
[16] V. Shiltsev et al., Phys. Rev. Lett. 99, 244801 (2007).
[17] G. Stancari et al., Phys. Rev. Lett. 107, 084802 (2011).
[18] X. Gu et al., Nucl. Instrum. and Methods A 743, pp. 56-67 (2014); X. Gu et al., Nucl. Instrum. and Methods A 798, pp. 36-43 (2015).
[19] R.C. Gupta et al., proc. 2011 Part. Accel. Conf., New York, NY, USA, pp. 1130-1132 (2011).
[20] P. Thieberger et al., 3*rd* International Beam Instrumentation Conference IBIC2014, Monterey, CA pp. 129-133 (2014).
[21] A.W. Chao, "Physics of collective beam instabilities in high energy accelerators", John Wiley & Sons, Chapter 5 (1993).

[22] P. Görgen, O. Boine-Frankenheim, and W. Fischer, Nucl. Instrum. and Methods A 777, pp. 43-53 (2015).